Journal of Atmospheric and Solar-Terrestrial Physics 179 (2018) 1–10

Contents lists available at ScienceDirect

Journal of Atmospheric and Solar-Terrestrial Physics

journal homepage: www.elsevier.com/locate/jastp

On the relationship between filaments and solar energetic particles

Ts Tsvetkov[a,*], R. Miteva[b], N. Petrov[a]

[a] Institute of Astronomy and National Astronomical Observatory, Bulgarian Academy of Sciences, 72 Tsarigradsko Chaussee Blvd. 1784, Sofia, Bulgaria
[b] Space Research and Technology Institute, Bulgarian Academy of Sciences, Acad. G. Bonchev Str., 1113 Sofia, Bulgaria

ARTICLE INFO

Keywords:
Solar activity
Filaments
Energetic particles
Protons

ABSTRACT

In the current study the association rate between solar energetic particles (protons) and filaments and/or filament eruptions (FEs) is investigated using the largest reported event sample. Proton events observed in the period 2010–2016 are accompanied by filaments in 92% (143/156) of the cases. Due to the lack of comprehensive catalog of all filaments, a catalog of FEs is used for the reversed association. Only 5% of FEs have in situ proton signatures with larger peak intensity, compared to the median of the entire proton sample. Other solar activity phenomena (flares and coronal mass ejections) related to the proton events show differences in their distributions compared to the respective FE-samples. The indication for a shock wave formation using the type II radio signatures is also considered and discussed.

1. Introduction

For more than a century now, the different aspects of solar activity are considered to be undoubtedly connected. All of them owe their existence to the magnetic field and represent different ways in which solar plasma is responding to the underlying magnetic field evolution (Priest, 2014). Solar eruptions with their variety of signatures of energy release including prominences, solar flares, coronal mass ejections (CMEs), radio emissions, fluxes of solar energetic particles (SEPs) and global waves, play a significant role in generating space weather. Large eruptions can evolve into CMEs that can plow through the solar wind and ultimately impact the Earth's magnetosphere (Munro et al., 1979; Gosling, 1993). Many of these CMEs were claimed to originate from prominence eruptions (Gopalswamy et al., 2003). Regardless of their magnitude, eruptions are key elements in figuring out the structure and dynamics of the solar atmosphere (Hurlburt, 2015).

Solar eruptions demonstrate the solar activity – they might be a simple local brightening or the most powerful event in our solar system. The easiest to observe are the bright chromospheric eruptions. Typically, they are visible in H_α and are evidence of some deep-seated disturbance which may manifest itself at widely separated points on the Sun (Richardson, 1937b). Observations of solar eruptive events at radio frequencies started a few years after the first detection of radio waves from an astronomical object in 1932 by Karl Jansky and often the radio bursts are associated with chromospheric eruptions (Newton and Barton, 1937; Richardson, 1937a).

The occurrence of solar eruption often happens after a disparition brusque (DB) of a filament. DBs are events observed in H_α, first reported by Deslandres in 1889 (Tandberg-Hanssen, 1995). They are a kind of filament eruptions (FEs) and may be a final or a temporary change in shape and visibility of the prominence (Raadu, Malherbe, Schmieder, Mein). Despite the terms prominence/filament show the location where the phenomenon is observed (limb/on-disk, respectively), they are used interchangeably in the current article. Nearly half of low-latitude filaments are seen to suffer a DB at least once during their existence (D'Azambuja, 1948). Two types of DBs are known – thermal (DBt (Mouradian et al., 1986)) and dynamical (DBd (Demoulin and Vial, 1992)). DBds are classical eruptions of a quiescent filament when the prominence plasma is ejected in the corona and in the heliosphere. In most of the cases DBds are final stage of prominence lifetime. The DBts on the other hand happen due to heating of the cold prominence material because of rising energy flux to the body of the filament. It disappears in H_α line, but becomes visible in ultraviolet or X-rays. Often the prominence appears again in H_α in a few hours when cooling down. The DBds are more often associated with CMEs and intense geomagnetic storms (Taliashvili, Mouradian, Páez; Schmieder et al., 2000; Gopalswamy et al., 2003).

CMEs consist of large structures containing plasma and magnetic fields that are expelled from the Sun into the heliosphere with the apparent speeds of the leading edges of CMEs range from about 20 to >2500 km s^{-1}, or from well below the sound speed in the corona to well above the Alfvèn speed (Webb and Howard, 2012; Chen, 2011). White-light observations reveal the typical structure of a CME: a bright loop with a dark cavity below and a core (Illing and Hundhausen, 1986) – structures that can also appear in the quiet solar atmosphere (Saito and Tandberg-Hanssen, 1973; Gibson et al., 2006). Although it is still

* Corresponding author.
E-mail address: tstsvetkov@astro.bas.bg (T. Tsvetkov).

https://doi.org/10.1016/j.jastp.2018.06.005
Received 24 February 2018; Received in revised form 1 June 2018; Accepted 7 June 2018

largely accepted that the CME core consists of a filament (House et al., 1981), some recent studies challenge this assumption and argue in favour of geometrical projection effects instead (Howard et al., 2017). Various studies explore the relation between different manifestations of solar activity. It was found that approximately half of active region (AR) FEs are associated with CMEs (Yan et al., 2011). Smaller eruptions may provide the ultimate source for the solar wind (Tian et al., 2014). As the FEs are claimed to be progenitors of mass ejections, different authors explore this relationship: 56% of eruptive prominences (EPs) are associated with CMEs by (Jing et al., 2004), or more than 80% by (Schmieder et al., 2012; Gopalswamy et al., 2003). CME-related are 92% of studied eruptive prominences by (Hori and Culhane, 2002), while the remaining 8% "show weak mass motions confined to nearby streamers".

While studying the relationship between different solar phenomena (Jing et al., 2004) divide FEs in two groups – active and quiescent. For a "solar flare" defined as the enhanced emission either in optical H_α or/ and in GOES X-ray, 41% of all prominence eruptions are linked with flares by (Jing et al., 2004). AR FEs are more likely to be associated with flares (95%) compared to quiescent FEs (28%). Similar results are obtained using larger samples by (Yan et al., 2011), connecting 96% of FEs with flares.

No statistical relationship has been reported between FEs and SEP fluxes (above 10 MeV). Previous studies discuss only isolated cases, e.g., single event studies are shown in (Hyder, 1967; Kahler et al., 1986; Kahler, 2001) and a handful of events are analyzed by (Kahler et al., 2015; Gopalswamy et al., 2015). Overall, the authors claimed that AR and impulsive phase are not necessary for the occurrence of the SEP events that were characterized by a rather steep power-law energy spectral index ($\gtrsim$4). CME-driven shock acceleration scenario was favored there, supported by the observation of IP type II radio bursts (without metric type II or shock-signatures formed only in the high corona).

The aim of this study is to re-evaluate the association between filaments and SEP events using larger event samples than before and the best quality prominence observations possible to date. Thus, the analysis covers the time period of Solar Dynamics Observatory (SDO (Pesnell et al., 2012)) mission. In Section 3.1 we present a list of SEP events observed from 2010 to the end of 2016 cross-checked for the appearance of a prominence. Due to the lack of comprehensive catalog of all observed prominences in the explored period to make the reverse association and look for filament-related SEP events, in Section 3.2 we used a list of all reported SDO FEs (McCauley et al., 2015). The association rate and characteristics of the filaments are finally compared with the respective properties of all FEs.

2. Observations and data analysis

For the analysis performed in this study, several different types of data and catalogs are used. The main components of the work are the prominences and SEP (with a focus on the proton) events.

2.1. Observational data

Space-based observations by the Atmospheric Imaging Assembly (AIA; (Lemen et al., 2012)) aboard the SDO are the main source for the prominence data analysis. We analyzed images from HeII 304 Å channel taken with spatial resolution of $\sim 1.5^{'}$ and a cadence of about 12 s. To check for possible association between the filaments and ARs we inspected images in AIA 1600 Å, 1700 Å and 4500 Å channels and the provided AR identification by https://solarmonitor.org.

In case we could not find associated filament in AIA observations, we checked H_α data archive from Big Bear Solar Observatory[1] or Kanzelhöhe Observatory.[2]

Observatoins from EUVI (Extreme Ultraviolet Imager) onboard STEREO (Solar TErrestrial RElations Observatory) A & B (Driesman et al., 2008) at the same wavelength (He II 304 Å) with spatial resolution of $\sim 1.6^{''}$ are used to ensure that behind the limb events not visible from AIA point of view are also considered.

Among the additional information relevant for the present study are the flare listing,[3],[4] radio burst identification (Miteva et al., 2018) and the SOHO/LASCO (Solar and Heliospheric Observatory/Large Angle and Spectrometric Coronagraph Experiment) CME Catalog[5] (Gopalswamy et al., 2009). Sunspot number data used for graphical representation of the solar cycle is taken from SILSO data archive, Royal Observatory of Belgium, Brussels.[6]

2.2. Selection of events

For the energetic proton events, data from the SOHO/ERNE[7] (Torsti et al., 1995) instrument is used. In the considered period (2010–2016), 186 proton events in the 17–22 MeV energy channel have been identified by visual inspection of the temporal profiles of the proton fluxes. A detailed report on the SOHO/ERNE 20 MeV catalog compilation is under way (for preliminary results see (Miteva et al., 2017)). Yearly distribution of all 186 SEP events is presented on Fig. 1.

Furthermore, we applied a temporal criteria for the association between the in situ proton event and the solar eruptive event, in terms of both solar flare and CME, where possible, similarly to the procedure summarized in (Miteva et al., 2018). For 111/186 (60%) of proton events both flare and CME could be identified, whereas for additional 45 proton cases only one of the eruptive event could be associated (due to data gaps, complex cases or high amount of uncertainty). For the remaining 30 proton cases, no solar origin association could be found and these events are not considered further in this study. Finally, a filament is sought at the time of onset of the solar flare/CME, regarded as the solar origin of the proton event.

In addition, a list of AIA/SDO FEs has already been compiled by (McCauley et al., 2015) and provided as online catalog[8] with $\gtrsim$900 entries over the period 2010–2014. Among all parameters listed in the catalog, relevant for our study are the onset and end times of the FE together with the related flare and CME. Based on these timings, we could associate the SOHO/ERNE proton event with the given FE.

The characteristics of the protons, filaments and related phenomena are summarized in Table 3 in the Appendix.

3. Results

3.1. Correlation analysis between solar proton events and filaments

Using the information for the proton-related flares and CMEs, we identified the presence or not of a filament (no distinction between eruptive or not). From our list, 143/156 SEP events were accompanied by prominences (92%), while in the remaining 13/156 cases (8%) could not be associated with any filaments.

The frequency of SEP occurrence increases around the solar maximum. (Fig. 1). The maximum of solar cycle 24 (as defined by sunspot number) reached in April 2014 coincides well with the maximum of registered proton events.

When evaluating the heliolocation of the proton origin, in addition to the information of the AR location taken from the proton-related

[1] http://www.bbso.njit.edu/pub/archive/.

[2] http://cesar.kso.ac.at/halpha3a/.

[3] https://hesperia.gsfc.nasa.gov/goes/goes_event_listings/.

[4] ftp://ftp.ngdc.noaa.gov/STP/SOLAR_DATA/SGD_PDFversion/.

[5] https://cdaw.gsfc.nasa.gov/CME_list/.

[6] http://sidc.be/silso/datafiles.

[7] https://srl.utu.fi/erne_data/.

[8] http://aia.cfa.harvard.edu/filament/.

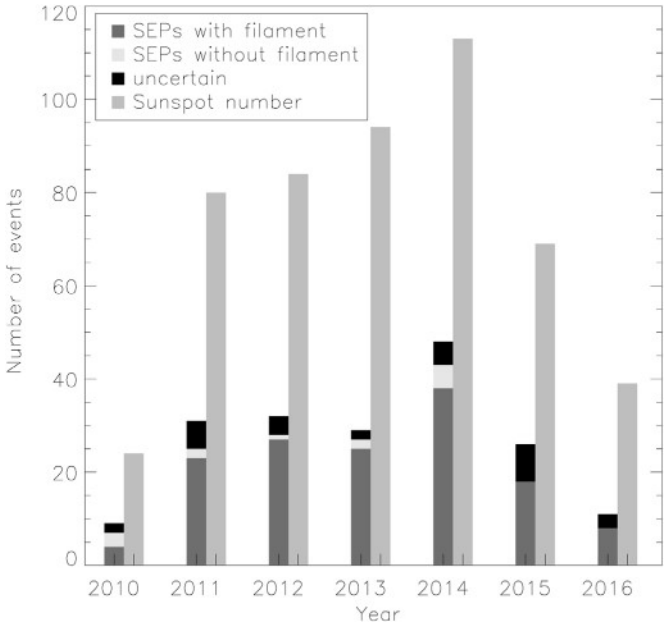

Fig. 1. Yearly distribution of all 186 proton events (left bar) using SOHO/ERNE data between 2010 and 2016 compared to the yearly mean total sunspot number (right bar). In different colors are separated SEP events accompanied (dark gray) or not (light gray) by filaments and those with unknown origin (black).

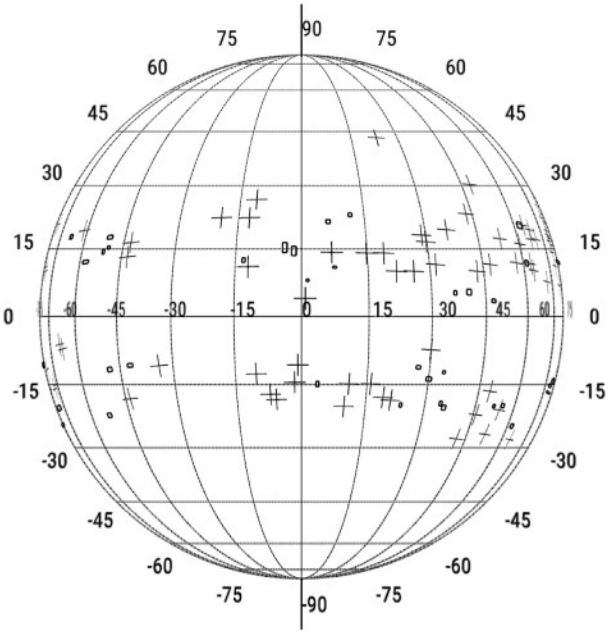

Fig. 2. Heliographic flare locations of 112 SEP events in the period 2010–2016 with known coordinates. Marked with crosses are all events observed before the solar maximum of cycle 24 (April 2014) and the events registered between April 2014 and the end of 2016 are marked with a rectangles.

flare, we also use the direction of propagation of the proton-related CME (given by the measurement position angle, MPA). For 156 proton events at least one manifestation of their solar origin (flare and/or CME) is identified. In 112 cases flare longitude and latitude are available (Fig. 2). For 40 additional events we successfully determined the hemisphere of their origin using the MPA of the related CME (north/south of the Equator or east/west of the central meridian). For the remaining 4 cases this procedure could not give accurate results since their location is either close to solar equator and/or central meridian.

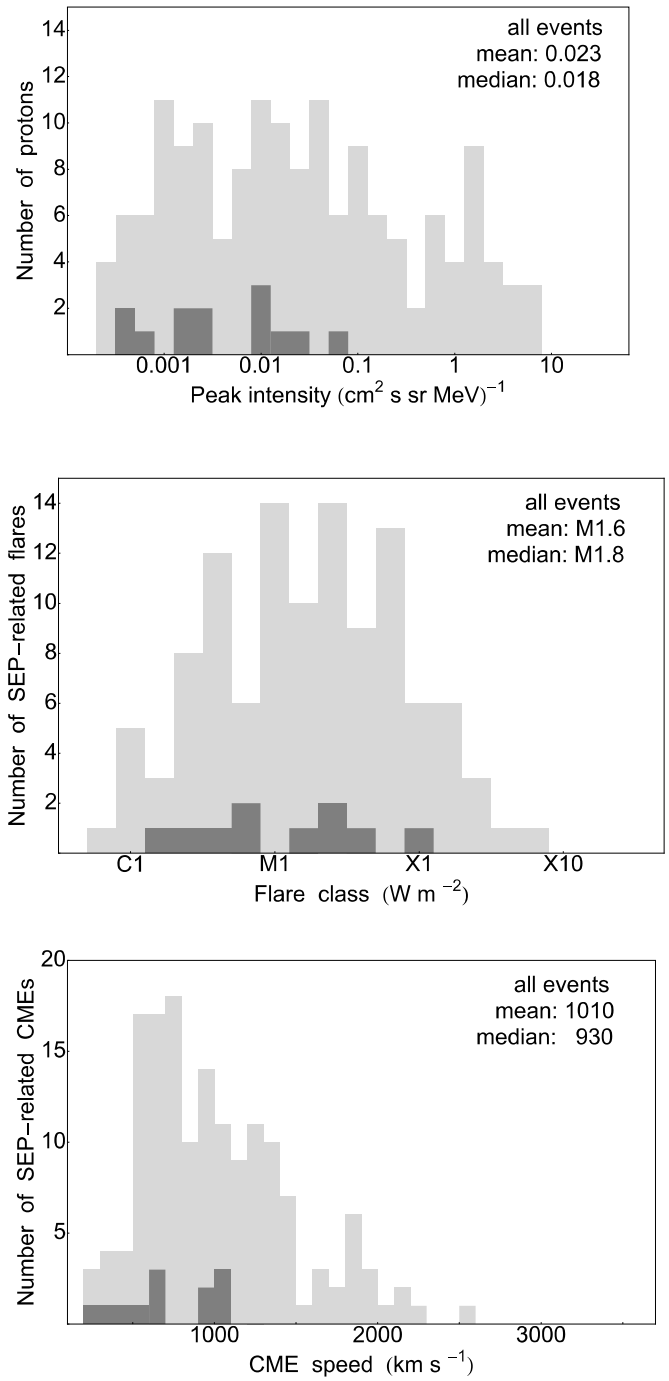

Fig. 3. Distributions of the proton sample and its solar origin: peak proton intensity (upper plot), flare class (middle) and CME speed (lower plot). In light gray are shown the events associated with filaments whereas in dark gray – without filaments. The sum of the two color bars gives the total number of events in each bin.

Due to these uncertainties the latter 44 events are not included on Fig. 2.

SEP events with identified origin and (flare) heliographic coordinates tend to appear in an area ± 30° around the solar equator, preferring latitudes around ± 15°. We obtain that 57% (86/152 cases) of the particle origin are observed north of the solar equator and 43% (66/152 cases) – to the south, confirming earlier studies for the solar cycle preference (Chandra et al., 2013). In addition, we mark that SEPs appear mostly in northern hemisphere before the maximum of solar cycle 24 (accepted here to be April 2014) and prefer southern

hemisphere after the solar maximum.

Moreover, we obtain that nearly 68% (103/152) of the proton sample originate from the western heliolongitudes, whereas the remaining 32% (49/152) are from the eastern. These percentages confirm the well-known observation for the preferential western origin of in situ observed particles.

Fig. 3 shows the stacked histograms of the protons and proton-related flares and CMEs. In different colors are given the events accompanied (light gray) or not by filaments (dark gray). On the upper plot is presented the distribution of the 156 proton events with respect to the peak intensity (in units of protons/(cm^2 s sr MeV)$^{-1}$). The mean/median values of the entire sample are 0.023/0.018 (cm^2 s sr MeV)$^{-1}$, respectively. The protons without filaments have lower intensities. In the middle plot is shown the flare class distribution with mean/median values – M1.6/M1.8, respectively, for the entire sample. The SEP-related flares without filaments range from classes C to X. The speed distribution of the SEP-related CME (lower plot) has mean/median values of 1010/930 km s^{-1}, respectively. The events without filaments tend to have lower speeds.

The association rate between SEP-related filaments and ARs is 88%. Only 17 (about 12%) of the 143 SEP-related prominences are not connected with AR.

Furthermore, we identified the type II burst occurrence (used as a proxy for a shock wave) to each reported proton case using as a guideline the timing of the flare and CME. Part of the associations are adopted from the catalog (Miteva et al., 2017), whereas the remaining cases are identified following the procedure described there. In total, 149 identifications were possible for the coronal range (in 87/149 of the cases, type II are present, denoted with "y" in Table 3). We found data for 152 cases in the IP range. In 97 of them IP type II could be identified ("Y"). From the entire list of 156 proton events, there are also a number of uncertain cases ("u") in either range, namely when no type II burst could be identified with certainty (7 in the coronal - 6 of them from the sample with filaments and 1 in the sample without filaments; 4 in the IP range - all of them from the sample with filaments). When we normalize to the event sample, we will drop the uncertain cases. Namely, in the case with filaments we normalize to 137 for the coronal type II and to 139 for the IP type II whereas in the case without filaments the coronal type II sample is normalized to 12 and the IP type II sample - to 13. Based on the possible identification, we summarize in Table 1 the occurrence or not of a coronal or IP type II radio burst with respect to the protons with and without filaments.

From the proton cases with filaments, 77 have identified radio signatures in the corona and 87 in the IP space. The results show that slightly more than a half of the proton events with filaments are accompanied by either coronal type II bursts (56%) or by IP type IIs (63%), see Table 1. When the proton events are not accompanied by filaments the majority of events are associated with type IIs. However, the explored sample consists of small amount of events.

As a rule, the above percentage in the coronal range is calculated independently on the findings in the IP one. However, one could impose different set of criteria on the appearance for the coronal and IP type II bursts. Requiring information for the type IIs to be known in both radio ranges, 145 cases remain from the entire proton sample. Among them, 135 (10) are for protons with (without) filaments.

When implying the condition of occurrence of both coronal and IP type II burst (noted with "yY" in column 7, Table 3), we obtain 45% (61/135) for the protons with filaments and 10% (1/10) for the protons without the presence of a filament. Furthermore, if we require a coronal type II that could not propagate through the IP space ("yN"), the results are 14%, 18/135 (with) and 30%, 3/10 (without). When no coronal but a presence only of IP signature is required ("nY"), we obtain 19%, 26/135 (10%, 1/10) for proton events with (without filaments), respectively. The remaining percentages (30 and 5 cases) are for the proton cases with lack of type II bursts in both radio ranges ("nN"), for the presence or not of filaments, respectively.

Table 1
Contingency table of the association rate between protons with/without filaments and the type II radio bursts occurring in the solar corona (using ground-based) and IP space (using satellite observations).

Proton-related sample	coronal type II		IP type II	
	Y	N	Y	N
with filaments	56% (77/137)	44% (60/137)	63% (87/139)	37% (52/139)
without filaments	83% (10/12)	17% (2/12)	77% (10/13)	23% (3/13)

3.2. Correlation analysis between FEs and solar proton events

The reverse case is to look for SEP event associations starting with a list of known filaments. However, no comprehensive list of all observed filaments during the period of interest is known to us. Nevertheless, a list of FEs is available and is used in this study, the AIA catalog of FEs (McCauley et al., 2015). The online version of the catalog[9] contains close to 980 entries in the period April 2010–October 2014, however only 954 are selected here for further analysis (after removal of double entries). Since this is not a list of all observed filaments (quiescent and eruptive), the reverse association is performed with the additional condition applied on the filaments to be eruptive. We checked our list of SEP-related filaments (see Table 3 in the Appendix) for the same period (2010–2014/10/19) and counted 114 SEP-related filaments registered - 81 in addition to (McCauley et al., 2015). Probably it is due to lack of eruption that these cases are not listed in AIA FE catalog, which means that the remaining 33 cases (listed in the catalog) are eruptive prominences. For the purpose of comparison as well as due to the large number of FEs and its availability, the AIA FE catalog is adopted here as a representative FE list.

The analysis starts with the timings provided for the FEs together with information about the identified accompanied solar features (flares, CMEs, ARs). Here, FEs and the proton events are assumed to be related phenomena if the onset of the proton as measured at 1 AU is either during the course of the FE or in given time window after the reported end of the FE. In order to allow time for particle acceleration and transport to the particle detector, especially for eastern events, we allow a delay of about 4 h. This value is close to the period between flare and proton onsets reported by (Miteva et al., 2018), e. g. 4.6/2.3 h mean/median value. From the reported FE duration and the onset time of the protons, we could identify only 51 cases that fulfill the above condition, or the probability of occurrence reaches only 5% (51/954). This number should be considered as a lower limit for the association rate, due to the adopted criterion for association and the omissions of filaments from the catalog.

Considering the reported FE classification in the AIA FE catalog (including the uncertain cases) the SEP-productive FEs are grouped as follows: 20/51 EPs originate from quiet Sun regions; 16/51 are AR FEs; only 1 of the EPs is located near solar equator; 4/51 - on intermediate latitudes; 7/51 EPs are polar crown type and 3 cases are not classified.

In Fig. 4 are shown the histograms of the FE-related protons, flares and CMEs. The distribution in terms of proton peak intensity of these FE-related protons is given on the upper plot. The mean/median value for the proton intensity is 0.042/0.022.

For comparative purposes, we give the flare and CME distributions of the respective FE-related samples, Fig. 4 (middle and lower plots). In this case, the obtained mean/median values of all events (plotted in light gray) are C2.7/C2.3 and 430/390 km s^{-1}, respectively. Much lower values (mean and median) for the FE-related flares and CMEs are

[9] http://aia.cfa.harvard.edu/filament/catalog_table.txt; status February 2018.

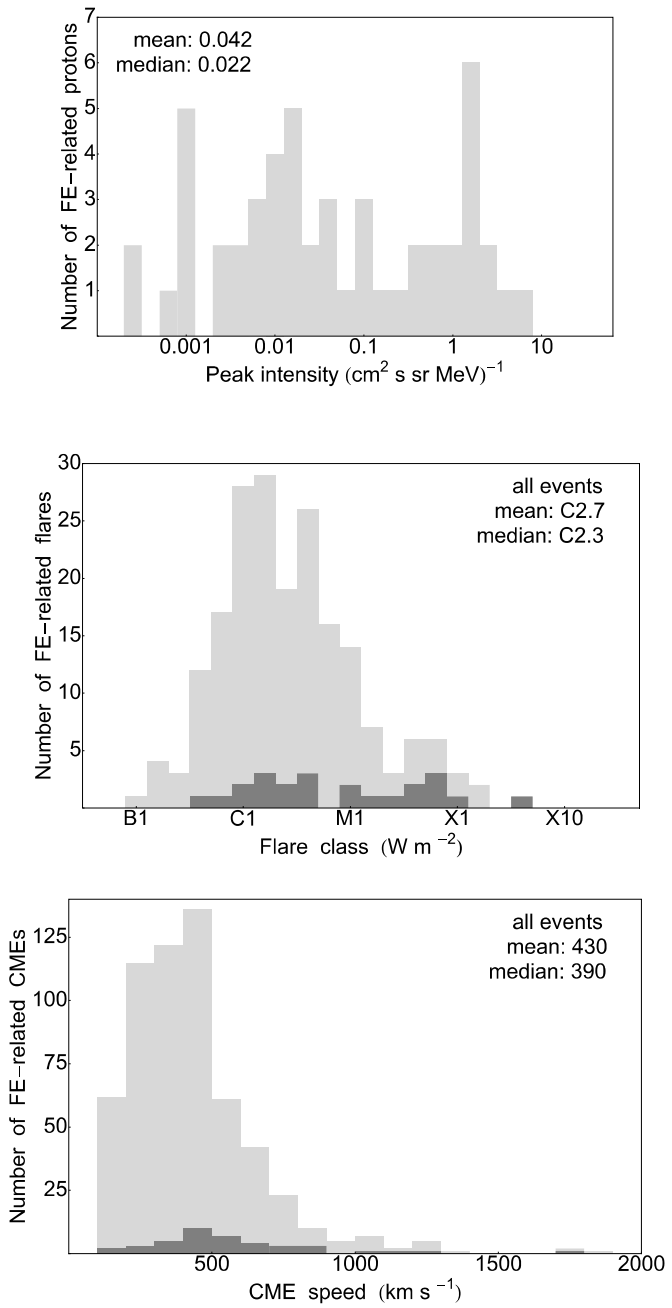

Fig. 4. Histogram of the intensity distribution of FE-related proton events (upper plot), flare class distribution of FE-related solar flares (middle) and speed distribution of FE-related CMEs (lower plot). In dark gray we mark the FE-related flares/CMEs, associated with SEP events.

obtained, compared to the respective values for the proton-related flare and CME samples (Fig. 3).

Furthermore, we plot (dark gray) the flare/CME distributions of the FE-related SEP sample. The mean/median values increase to C8.9/C6.9 and 570/510 km s^{-1}, respectively. As expected, the sources of SEPs are among the more powerful solar eruptive events.

The statistical difference between the proton-related and FE-related samples is investigated using the Kolmogorov-Smirnov test. The results are shown in Table 2. The proton list and FE-proton list is the only pair that could be drawn from the same parent distribution within the 5% confidence level, adopted here. For the pairs of proton-related and FE-related flare and CME distributions, however, we readily obtain statistical difference. Namely, the proton-related flares and those in association to FEs comprise two different distributions. Similar result is obtained for the two CME samples. Both, the proton-related flares and CMEs are of larger magnitude, compared to the respective FE-related samples.

Table 2
Table of statistical difference under the Kolmogorov-Smirnov test. A statistical difference between two samples of events is considered when the calculated probability (D) is larger than the reference value for the selected here 5% confidence level, $D_{0.05} = 1.36[(n_1 + n_2)/n_1{*}n_2]^{0.5}$, where n_1 and n_2 are the number of events in the two distributions.

	Proton-related (n_1) and FE-related samples (n_2)		
	protons	flares	CMEs
difference probability	No D=0.12; $D_{0.05}$=0.22	Yes D = 0.49; $D_{0.05}$ = 0.16	Yes D = 0.68; $D_{0.05}$ = 0.12
sample size	n_1=156; n_2=51	n_1 = 112; n_2 = 197	n_1 = 155; n_2 = 595

4. Conclusions and discussions

We present the most detailed statistical study to date about the connection between solar energetic protons and filaments relying on space-based observations by SDO, STEREO A & B, SOHO and ground-based H_α telescopes in Big Bear Solar Observatory or Kanzelhöhe Observatory. We inspected 156 proton events in the period between 2010 and the end of 2016 to identify the related solar activity phenomena (including prominences, flares, coronal mass ejections, radio bursts of type II, etc.). The main results are summarized below:

- Filament-related proton events tend to be significantly more common than non-related - 143-to-13 out of 156 cases (92-to-8%).
- More SEP events appeared in northern solar hemisphere than in southern for the studied time period - 86-to-66 out of 152 cases (57-to-43%). The preferred solar hemisphere changes at the year of maximum of solar cycle 24 – in the years before April 2014 more SEP events are observed north of solar equator, while the dependency changes in the second half of the period.
- SEP events originate from a region not farther than ± 30° around the solar equator. The largest amount of events are detected to originate on about ± 15° latitude. The FE-related SEPs, however, have a broader latitudinal distribution including 7 events that originate at polar regions.
- The majority of the SEPs in the considered period are associated with the western hemisphere solar activity (103/156 cases or close to 68%).
- 126 out of 143 SEP-related filaments (88%) are localized in active regions. The remaining 12% consists of only 17 cases for 6 years. The reported cases of prominences outside active regions producing SEP event are rare, such as the events presented by (Kahler et al., 2015; Gopalswamy et al., 2015). Two of the reported there events are also listed in the current study (2011/11/26 and 2013/09/29). The one from 2011 is categorized as SEP-related filament out of active region by (Gopalswamy et al., 2015), however, we link the filament eruption with AR11353.
- We found that only 51/954 (5%) of the cataloged eruptive filaments tend to produce SEP events.
- Proton events with filaments show a tendency to be accompanied by coronal (56%) and/or IP type II bursts (63%). Among the protons with filaments, 45% have type II features in both ranges, 14% have shock signatures only in the coronal range, 19% – only in the IP range, and the remaining 22% is for the lack of any type II bursts.

Filament-related SEP events tend to show higher peak intensities than the non-related ones. Even higher peak proton intensities are

obtained when the SEPs are associated with FEs, however, the two samples are statistically the same. In contrast, flares/CMEs are statistically different populations when associated with proton or FE sample. Proton-related flare and/or CME distributions have larger mean/median class and/or speed compared to the respective flares and/or CMEs of the FE-related SEP samples. Thus, the FEs influence indirectly on the SEP events through a subset of stronger flares/CMEs. The occurence of type II signatures in the presence of filaments does not seem to differ from the overall case (Miteva et al., 2017): reports 73 ± 10% IP type IIs and 59 ± 9% coronal type IIs related to protons for the period of solar cycle 24, while our study shows 63% and 56%, respectively.

Further analysis in several aspects is already under way. The proton catalog (SOHO/ERNE 17–22 MeV) over the previous solar cycle 23 is under completion, allowing the current analysis to be also extended. In addition, the kinematics of the filaments, where permissible to be evaluated by the available observations, will be explored in details. Finally, the filament evolution together with the spectral index characteristics of the filament-related proton events will be the topic of a separate study reported elsewhere.

Acknowledgement

This work was supported by National Science Fund of Bulgaria with grant DN 08-1/2016 and contract No. DNTS/Russia 01/6 (23-Jun-2017).

Appendix A. Supplementary data

Supplementary data related to this article can be found at http://dx.doi.org/10.1016/j.jastp.2018.06.005.

Appendix

Table 3 lists the SOHO/ERNE 20 MeV proton events and selected parameters of the proton-associated flares, CMEs, filaments and type II radio bursts, using ground-based observations for the coronal signatures and space-borne for the IP features. When a filament has been identified in relation to the proton event, we list the active region (AR) intersected by this filament and whether it is listed in the catalog of filament eruptions (McCauley et al., 2015). In case of inability to define some characteristic or possible association for the events we use designation 'u' for uncertainty, while 'g' stands for gap in the data archive of current instrument.

Table 3
Table of ~20 MeV SOHO/ERNE proton events (2010–2016) and associated solar events: flares (class/onset), CMEs (time of first appearance/linear speed), filaments (Y/N and related AR), appearance of type II radio burst (in the corona: y/n, in the IP space: Y/N), whether the filament is listed in (McCauley et al., 2015) (Y/N). Time in UT; speed in km s^{-1}. Abbreviations: g: data gap; n/N: no; u: uncertain; y/Y: yes.

Proton onset		Solar flare	CME	Filaments		Type	Listed
yyyy/mm/dd	hr	class/onset	time/speed	Y/N	AR	II	Y/N
2010/02/12	17	M8.3/11:19	u	N	–	yN	–
2010/06/12	3	M2.0/00:30	01:32/486	N	–	yY	–
2010/08/14	11	C4.4/09:38	10:12/1205	Y	11097	yY	N
2010/08/18	7	C4.5/04:45	05:48/1471	Y	11098	yY	N
2010/08/31	23	u	21:17/1304	Y	Y	nY	N
2010/09/08	25	C3.3/23:05	23:27/818	Y	11105	nY	N
2010/12/31	6	C1.3/04:18	05:00/363	N	–	yN	–
2011/01/28	2	M1.3/00:44	01:26/606	Y	11149	yY	Y
2011/02/15	4	X2.2/01:44	02:24/669	Y	11158	yY	Y
2011/03/07	17	C5.8/14:46	15:50/698	Y	11163	yY	N
2011/03/07	22	M3.7/19:43	20:00/2125	Y	11164	yY	Y
2011/03/16	22	C3.7/17:52	19:12/682	Y	11166/11169	uN	N
2011/03/21	5	u	02:24/1341	Y	11174	yY	N
2011/03/29	22	u	20:36/1264	Y	11180/11183	nN	Y
2011/05/11	4	B8.1/02:23	02:48/745	Y	11203/11205	yY	Y
2011/06/04	12	u	06:48/1407	Y	Y	nY	N
2011/06/07	9	M2.5/06:16	06:49/1255	Y	11233	yY	Y
2011/06/11	13	u	12:00/522	Y	N	nN	Y
2011/08/02	7	M1.4/05:19	06:36/712	Y	11261	yY	N
2011/08/03	15	M6.0/13:17	14:00/610	Y	11261	yY	N
2011/08/04	6	M9.3/03:41	04:12/1315	Y	11261	yY	Y
2011/08/08	19	M3.5/18:00	18:12/1343	Y	11261/11263	yY	N
2011/08/09	9	X6.9/07:48	08:12/1610	Y	11263	yY	N
2011/09/04	6	C9.0/04:36	05:12/262	Y	11280	yN	N
2011/09/04	32	C7.9/23:58	00:48/622	N	–	nN	–
2011/09/06	3	M5.3/01:35	02:24/782	Y	11283	yY	Y
2011/09/07	2	X2.1/22:12	23:05/575	Y	11283	yY	Y
2011/09/21	24	u	22:12/1007	N	–	nN	–
2011/10/22	12	M1.3/10:00	10:24/1005	Y	11314	nY	N
2011/11/03	24	M2.1/23:28	23:30/991	Y	11330/11333	nY	N

(continued on next page)

Table 3 (*continued*)

Proton onset		Solar flare	CME	Filaments		Type	Listed
yyyy/mm/dd	hr	class/onset	time/speed	Y/N	AR	II	Y/N
2011/11/17	8	u	20:36/1041	Y	11353	nY	N
2011/11/26	9	C1.2/06:09	07:12/933	Y	11353	nY	Y
2012/01/19	19	M3.2/13:44	14:36/1120	Y	11402	nY	Y
2012/01/27	20	C2.4/14:31	15:13/2508	Y	N	yY	–
2012/02/24	5	u	03:46/800	Y	N	nY	–
2012/03/04	19	M2.0/10:29	11:00/1306	Y	11429	nY	N
Proton onset		Solar flare	CME	EP		Type	Listed
yyyy/mm/dd	hr	class/onset	time/speed	Y/N	AR	II	Y/N
2012/03/07	7	X1.3/01:05	01:30/1825	Y	11429/11430	yY	N
2012/03/13	19	M7.9/17:12	17:36/1884	Y	11429	nY	N
2012/03/29	31	B6.2/23:19	23:36/753	Y	11442	nN	Y
2012/04/05	24	C1.5/20:49	21:25/828	Y	11450	yY	Y
2012/04/09	15	C3.9/12:12	12:36/921	Y	11452	yY	Y
2012/04/18	42	C1.8/14:42	15:12/540	Y	11462	nN	N
2012/04/20	3	B9.0/01:55	02:00/345	Y	11463	nN	N
2012/05/17	3	M5.1/01:25	01:48/1582	Y	11476	yY	Y
2012/05/26	22	u	20:58/1966	Y	11484	yY	N
2012/06/02	7	C1.5/04:15	04:36/1175	Y	Y	nN	N
2012/06/08	7	C7.7/02:51	03:47/353	Y	11494	yN	Y
2012/06/12	11	u	05:24/864	Y	11494/11499	nN	N
2012/06/14	17	M1.9/12:52	14:12/987	Y	11505	nY	N
2012/07/06	24	X1.1/23:01	23:24/1828	Y	11515	yY	N
2012/07/12	18	X1.4/15:37	16:48/885	Y	11520	yY	N
2012/07/17	16	M1.7/12:03	13:48/958	Y	N	nY	N
2012/07/19	9	M7.7/04:17	05:24/1631	Y	11520	yY	N
2012/07/23	8	u	02:36/2003	Y	11523	yY	Y
2012/08/31	23	C8.4/19:45	20:00/1442	Y	Y	nY	Y
2012/09/08	12	g	10:00/734	Y	11562/11564	nY	N
2012/09/21	12	u	06:24/639	N	–	nN	–
2012/09/27	g	C3.7/23:36	24:12/947	Y	11575/11577	yY	Y
2012/10/07	16	u	07:36/663	Y	N	nN	N
2012/11/08	g	u	11:00/972	Y	Y	nY	N
2013/02/06	16	C8.7/00:04	00:24/1867	Y	11667	yN	Y
2013/02/26	13	u	09:12/987	Y	11675	nY	N
2013/03/05	14	u	03:48/1316	Y	Y	nY	N
2013/03/15	18	M1.1/05:46	07:12/1063	Y	11692	nY	N
2013/04/11	8	u	07:24/861	Y	11719	yY	N
2013/04/21	11	u	07:24/919	N	–	nu	–
2013/04/24	24	C1.2/21:50	22:12/594	Y	11723	nN	N
2013/05/02	9	M1.1/04:58	05:24/671	Y	11731	yN	N
2013/05/13	20	X2.8/15:48	16:08/1850	Y	11745	yY	N
2013/05/15	10	X1.2/01:25	01:48/1366	Y	11738	yY	Y
2013/05/22	15	M5.0/13:08	12:26/1466	Y	11745	yY	N
2013/06/21	13	M2.9/02:30	03:12/1900	Y	11777	nY	N
2013/06/28	8	C4.4/01:36	02:00/1037	N	–	nY	–
2013/08/17	21	M3.3/18:16	19:12/1202	Y	11818	yY	Y
2013/08/20	5	u	08:12/784	Y	N	nN	N
2013/08/30	7	C8.3/02:04	02:48/949	Y	11836	yY	N
Proton onset		Solar flare	CME	EP		Type	Listed
yyyy/mm/dd	hr	class/onset	time/speed	Y/N	AR	II	Y/N
2013/09/24	32	u	20:36/919	Y	N	nN	Y
2013/09/29	43	C1.2/21:43	22:12/1179	Y	N	yY	Y
2013/10/11	19	M1.5/07:01	07:24/1200	Y	N	yY	N
2013/10/22	24	M4.2/21:15	21:48/459	Y	11873/11875	yY	N
2013/10/25	13	X2.1/14:51	15:12/587	Y	11882	yY	N

(*continued on next page*)

Table 3 (*continued*)

Proton onset		Solar flare	CME	EP		Type	Listed
yyyy/mm/dd	hr	class/onset	time/speed	Y/N	AR	II	Y/N
2013/10/28	7	M5.1/04:32	04:48/1201	Y	11875	yY	Y
2013/12/07	12	M1.2/07:17	07:36/1085	Y	Y	yY	N
2013/12/12	6	C4.6/03:11	03:36/1002	Y	11912	yY	N
2013/12/13	29	u	21:24/518	Y	Y	nN	N
2013/12/26	8	u	03:34/1336	Y	Y	nY	N
2013/12/28	20	C9.3/17:53	17:36/1118	Y	11936	nY	N
2014/01/04	23	M4.0/18:47	21:23/977	N	–	nN	–
2014/01/06	9	u	08:00/1402	Y	11937/11938	yY	Y
2014/01/07	21	X1.2/18:04	18:24/1830	Y	11943/11944	yY	N
2014/01/20	31	C3.6/21:39	22:00/721	Y	Y	nY	N
2014/01/21	20	M1.3/18:57	18:48/1035	N	–	uN	–
2014/02/11	15	C8.4/13:15	13:48/330	Y	11974	yN	N
2014/02/11	24	u	19:24/613	Y	11975	uY	N
2014/02/14	13	u	08:48/1165	Y	11974	nN	N
2014/02/16	11	M1.1/09:20	10:00/634	Y	11977	nu	N
2014/02/18	5	C3.3/09:49	01:36/779	Y	N	yN	Y
2014/02/20	8	M3.0/07:26	08:00/948	Y	Y	yY	N
2014/02/25	5	X4.9/00:39	01:26/2147	Y	11990	yY	Y
2014/03/22	13	u	10:00/756	Y	12005	nN	N
2014/03/24	12	u	07:12/809	Y	Y	nN	N
2014/03/28	25	M2.6/23:44	23:48/514	Y	12017	yY	N
2014/03/29	19	X1.0/17:35	18:12/528	Y	12017/12018	yY	N
2014/04/02	25	M6.5/13:18	13:36/1471	Y	12027	yY	Y
2014/04/05	4	u	06:24/798	Y	12021	nN	N
2014/04/18	14	M7.3/12:31	13:26/1203	Y	Y	yY	N
2014/04/25	2	X1.3/00:17	00:48/456	Y	12046	yN	N
2014/05/07	19	M1.2/16:07	16:24/923	Y	12055/12056	nY	N
2014/05/09	4	u	02:48/1099	Y	12049	yY	Y
2014/06/06	13	u	12:48/704	Y	N	yN	N
2014/06/12	25	M3.1/21:34	22:12/684	Y	12085	yY	N
2014/06/17	17	C3.0/08:13	09:12/1198	Y	12093/12094	nN	N
2014/07/08	18	M6.5/16:06	16:36/773	Y	12113	yN	Y
2014/08/22	13	u	11:12/600	Y	12139	yY	N
2014/08/25	18	M2.0/14:46	15:36/55	Y	Y	yY	N
2014/08/29	3	u	17:24/766	Y	N	uN	N
Proton onset		Solar flare	CME	EP		Type	Listed
yyyy/mm/dd	hr	class/onset	time/speed	Y/N	AR	II	Y/N
2014/09/02	5	u	11:12/1901	Y	N	yY	Y
2014/09/10	26	X1.6/17:21	18:00/1267	Y	12158	yY	N
2014/09/22	9	u	06:12/618	Y	N	nY	N
2014/09/24	30	u	21:30/1350	Y	N	yY	N
2014/10/02	21	M7.3/18:49	19:12/513	Y	12173	yN	N
2014/10/10	19	C3.0/15:42	16:12/782	Y	12182	nN	N
2014/10/13	4	u	00:12/521	Y	12184	nN	N
2014/10/15	24	M2.2/19:07	18:48/848	Y	12129	uN	N
2014/11/01	9	C2.7/04:44	05:00/1628	Y	12200	yu	–
2014/11/07	6	M2.0/04:12	04:38/672	N	–	nu	–
2014/11/09	14	u	10:24/633	Y	12207	nN	–
2014/11/10	11	C7.6/02:18	03:36/230	N	–	nN	–
2014/12/05	8	C2.1/05:28	06:24/534	N	–	yN	–
2014/12/13	11	g	14:24/2222	Y	12227	yY	–
2015/02/21	11	u	09:24/1120	Y	N	nN	–
2015/04/12	26	C6.4/23:24	23:48/678	Y	12320	yN	–
2015/04/14	15	u	02:36/1198	Y	12321	yN	–
2015/05/06	15	M1.9/11:45	12:12/738	Y	12329	yN	–
2015/05/12	5	C2.6/02:15	02:48/772	Y	12335/12337	yN	–
2015/06/14	8	C5.9/03:48	04:12/1228	Y	12365	nN	–

(*continued on next page*)

Table 3 (*continued*)

Proton onset		Solar flare	CME	EP		Type	Listed
yyyy/mm/dd	hr	class/onset	time/speed	Y/N	AR	II	Y/N
2015/06/18	4	M1.2/00:33	01:26/1714	Y	12365	nN	–
2015/06/21	19	M2.6/02:06	02:36/1366	Y	12371	yY	–
2015/07/01	16	u	14:36/1435	Y	N	uY	–
2015/07/19	12	C2.1/09:22	09:48/782	Y	12384	nN	–
2015/08/24	10	M5.6/07:26	08:48/272	Y	12403	nN	–
2015/09/20	19	M2.1/17:32	18:12/1239	Y	12418	yY	–
2015/09/30	19	g	09:36/586	Y	12422	nN	–
2015/10/22	7	C4.4/02:13	03:12/817	Y	12434	nN	–
2015/10/29	3	u	02:36/530	Y	12437	yY	–
2015/11/04	16	M3.7/13:31	14:48/578	Y	12443	yY	–
2015/11/09	22	M3.9/12:49	13:25/1041	Y	12449	yY	–
2015/12/28	14	M1.8/11:20	12:12/1212	Y	12472	nY	–
2016/01/01	24	M2.3/23:10	23:24/1730	Y	12473	yN	–
2016/01/28	13	C9.6/11:48	12:24/562	Y	12488	nN	–
2016/01/29	24	C2.0/20:48	22:12/800	Y	12488	nN	–
2016/02/11	27	C8.9/20:18	21:18/719	Y	12497	yN	–
2016/03/16	8	C2.2/06:34	07:00/592	Y	12522	yN	–
2016/04/18	27	M6.7/00:14	00:48/1084	Y	Y	yN	–
2016/05/15	17	C3.2/15:19	15:12/1118	Y	12544	uN	–
2016/07/20	25	C4.6/22:03	23:12/426	Y	12565/12657	nN	–

References

D'Azambuja, L., 1948. Thesis at the Observatory of Paris. PhD thesis. pp. 1948.

Chandra, R., Gopalswamy, N., Mäkelä, P., Xie, H., Yashiro, S., Akiyama, S., Uddin, W., Srivastava, A.K., Joshi, N.C., Jain, R., Awasthi, A.K., Manoharan, P.K., Mahalakshmi, K., Dwivedi, V.C., Choudhary, D.P., Nitta, N.V., Dec. 2013. Solar energetic particle events during the rise phases of solar cycles 23 and 24. Adv. Space Res. 52, 2102–2111.

Chen, P.F., Apr. 2011. Coronal mass ejections: models and their observational basis. Living Rev. Sol. Phys. 8, 1.

Demoulin, P., Vial, J.C., Oct. 1992. Structural characteristics of eruptive prominences. Sol. Phys. 141, 289–301.

Driesman, A., Hynes, S., Cancro, G., Apr. 2008. The STEREO observatory. Space Sci. Rev. 136, 17–44.

Gibson, S.E., Foster, D., Burkepile, J., de Toma, G., Stanger, A., Apr. 2006. The calm before the storm: the link between quiescent cavities and coronal mass ejections. Astrophys. J. 641, 590–605.

Gopalswamy, N., Shimojo, M., Lu, W., Yashiro, S., Shibasaki, K., Howard, R.A., Mar. 2003. Prominence eruptions and coronal mass ejection: a statistical study using microwave observations. Astrophys. J. 586, 562–578.

Gopalswamy, N., Yashiro, S., Michalek, G., Stenborg, G., Vourlidas, A., Freeland, S., Howard, R., Apr. 2009. The SOHO/LASCO CME catalog. Earth Moon Planets 104, 295–313.

Gopalswamy, N., Mäkelä, P., Akiyama, S., Yashiro, S., Xie, H., Thakur, N., Kahler, S.W., June 2015. Large solar energetic particle events associated with filament eruptions outside of active regions. Astrophys. J. 806, 8.

Gosling, J.T., Nov. 1993. The solar flare myth. J. Geophys. Res. 98, 18937–18950.

Hori, K., Culhane, J.L., Feb. 2002. Trajectories of microwave prominence eruptions. Astron. Astrophys. 382, 666–677.

House, L.L., Wagner, W.J., Hildner, E., Sawyer, C., Schmidt, H.U., Mar. 1981. Studies of the corona with the solar maximum mission coronagraph/polarimeter. Astrophys. J. Lett. 244, L117–L121.

Howard, T.A., DeForest, C.E., Schneck, U.G., Alden, C.R., Jan. 2017. Challenging some contemporary views of coronal mass ejections. II. The case for absent filaments. Astrophys. J. 834, 86.

Hurlburt, N., Dec. 2015. Automated detection of solar eruptions. Journal of Space Weather and Space Climate 5 (27), A39.

Hyder, C.L., July 1967. A phenomenological model for disparitions brusques followed by flarelike chromospheric brightenings, I: the model, its consequences, and observations in quiet solar regions. Sol. Phys. 2, 49–74.

Illing, R.M.E., Hundhausen, A.J., Oct. 1986. Disruption of a coronal streamer by an eruptive prominence and coronal mass ejection. J. Geophys. Res. 91, 10951–10960.

Jing, J., Yurchyshyn, V.B., Yang, G., Xu, Y., Wang, H., Oct. 2004. On the relation between filament eruptions, flares, and coronal mass ejections. Astrophys. J. 614, 1054–1062.

Kahler, S.W., 2001. Origin and properties of solar energetic particles in space. Washington DC American Geophysical Union Geophysical Monograph Series 125, 109–122.

Kahler, S.W., Cliver, E.W., Cane, H.V., McGuire, R.E., Stone, R.G., Sheeley Jr., N.R., Mar. 1986. Solar filament eruptions and energetic particle events. Astrophys. J. 302, 504–510.

Kahler, S., Gopalswamy, N., Makela, P., Akiyama, S., Yashiro, S., Xie, H., Thakur, N., July 2015. Filament eruptions outside of active regions as sources of large solar energetic particle events. In: 34th International Cosmic Ray Conference (ICRC2015), Volume 34 of International Cosmic Ray Conference, pp. 48.

Lemen, J.R., Title, A.M., Akin, D.J., Boerner, P.F., Chou, C., Drake, J.F., Duncan, D.W., Edwards, C.G., Friedlaender, F.M., Heyman, G.F., Hurlburt, N.E., Katz, N.L., Kushner, G.D., Levay, M., Lindgren, R.W., Mathur, D.P., McFeaters, E.L., Mitchell, S., Rehse, R.A., Schrijver, C.J., Springer, L.A., Stern, R.A., Tarbell, T.D., Wuelser, J.-P., Wolfson, C.J., Yanari, C., Bookbinder, J.A., Cheimets, P.N., Caldwell, D., Deluca, E.E., Gates, R., Golub, L., Park, S., Podgorski, W.A., Bush, R.I., Scherrer, P.H., Gummin, M.A., Smith, P., Auker, G., Jerram, P., Pool, P., Soufli, R., Windt, D.L., Beardsley, S., Clapp, M., Lang, J., Waltham, N., Jan. 2012. The atmospheric imaging assembly (aia) on the solar dynamics observatory (SDO). Sol. Phys. 275, 17–40.

McCauley, P.I., Su, Y.N., Schanche, N., Evans, K.E., Su, C., McKillop, S., Reeves, K.K., June 2015. Prominence and filament eruptions observed by the solar dynamics observatory: statistical properties, kinematics, and online catalog. Sol. Phys. 290, 1703–1740.

Miteva, R., Samwel, S.W., Costa-Duarte, M.V., Feb. 2018. The wind/EPACT proton event catalog 1996-2016. Sol. Phys. 293, 27.

Miteva, R., Samwel, S.W., Krupar, V., Dec. 2017. Solar energetic particles and radio burst emission. Journal of Space Weather and Space Climate 7 (27), A37.

Mouradian, Z., Martres, M.J., Soru-Escaut, I., Dec. 1986. The heating of filaments as a disappearance process. In: Poland, A.I. (Ed.), NASA Conference Publication, Volume 2442 of *NASA Conference Publication*.

Munro, R.H., Gosling, J.T., Hildner, E., MacQueen, R.M., Poland, A.I., Ross, C.L., Feb. 1979. The association of coronal mass ejection transients with other forms of solar activity. Sol. Phys. 61, 201–215.

Newton, H.W., Barton, H.J., June 1937. Bright solar eruptions and radio fadings during the years 1935-36. Mon. Not. Roy. Astron. Soc. 97, 594.

Pesnell, W.D., Thompson, B.J., Chamberlin, P.C., Jan. 2012. The solar dynamics observatory (SDO). Sol. Phys. 275, 3–15.

Priest, E., May 2014. Magnetohydrodynamics of the Sun. Cambridge University Press.

Raadu, M.A., Malherbe, J.M., Schmieder, B., Mein, P., Sept. 1987. Material ejecta in a disturbed solar filament. Sol. Phys. 109, 59–79.

Richardson, R.S., Apr. 1937a. Relation between bright chromospheric eruptions and fade-Outs of high-frequency radio transmission. Publ. Astron. Soc. Pac. 49, 82.

Richardson, R.S., Oct. 1937b. The nature of bright chromospheric eruptions. Publ. Astron. Soc. Pac. 49, 233–239.

Saito, K., Tandberg-Hanssen, E., July 1973. The arch systems, cavities, and prominences in the helmet streamer observed at the solar eclipse, november 12, 1966. Sol. Phys. 31, 105–121.

Schmieder, B., Delannée, C., Yong, D.Y., Vial, J.C., Madjarska, M., June 2000. Multi-wavelength study of the slow "disparition brusque" of a filament observed with SOHO. Astron. Astrophys. 358, 728–740.

Schmieder, B., Demoulin, P., Aulanier, G., July 2012. Title. In: 39th COSPAR Scientific Assembly, Volume 39 of COSPAR Meeting, pp. 1.

Taliashvili, L., Mouradian, Z., Páez, J., Sept. 2009. Dynamic and thermal disappearance of

prominences and their geoeffectiveness. Sol. Phys. 258, 277–295.
Tandberg-Hanssen, E. (Ed.), 1995. The Nature of Solar Prominences, vol. 199 of Astrophysics and Space Science Library.
Tian, H., DeLuca, E.E., Cranmer, S.R., De Pontieu, B., Peter, H., Martínez-Sykora, J., Golub, L., McKillop, S., Reeves, K.K., Miralles, M.P., McCauley, P., Saar, S., Testa, P., Weber, M., Murphy, N., Lemen, J., Title, A., Boerner, P., Hurlburt, N., Tarbell, T.D., Wuelser, J.P., Kleint, L., Kankelborg, C., Jaeggli, S., Carlsson, M., Hansteen, V., McIntosh, S.W., Oct. 2014. Prevalence of small-scale jets from the networks of the solar transition region and chromosphere. Science 346 (27), 1255711.
Torsti, J., Valtonen, E., Lumme, M., Peltonen, P., Eronen, T., Louhola, M., Riihonen, E., Schultz, G., Teittinen, M., Ahola, K., Holmlund, C., Kelhä, V., Leppälä, K., Ruuska, P., Strömmer, E., Dec. 1995. Energetic particle experiment erne. Sol. Phys. 162, 505–531.
Webb, D.F., Howard, T.A., June 2012. Coronal mass ejections: observations. Living Rev. Sol. Phys. 9, 3.
Yan, X.-L., Qu, Z.-Q., Kong, D.-F., July 2011. Relationship between eruptions of active-region filaments and associated flares and coronal mass ejections. Mon. Not. Roy. Astron. Soc. 414, 2803–2811.